

## Atomic-Scale Roughness Effect on Capillary Force in Atomic Force Microscopy

Joonkyung Jang,<sup>\*,†</sup> M. A. Ratner,<sup>‡</sup> and George C. Schatz<sup>\*,‡</sup>

*School of Nano Science & Technology, Pusan National University, Busan 609-735, South Korea, and  
Department of Chemistry, Northwestern University, Evanston, Illinois 60208-3113*

*Received: November 13, 2005; In Final Form: December 11, 2005*

We study the capillary force in atomic force microscopy by using Monte Carlo simulations. Adopting a lattice gas model for water, we simulated water menisci that form between a rough silicon-nitride tip and a mica surface. Unlike its macroscopic counterpart, the water meniscus at the nanoscale gives rise to a capillary force that responds sensitively to the tip roughness. With only a slight change in tip shape, the pull-off force significantly changes its qualitative variation with humidity.

In a typical atomic force microscopy (AFM) experiment, a water meniscus forms between the AFM tip and sample surfaces. This meniscus at the nanoscale produces a capillary force that governs the force (image) measured in AFM.<sup>1–3</sup> So far, prediction of the meniscus shape and the resulting capillary force has relied heavily on thermodynamic theories such as the Kelvin equation.<sup>4,5</sup> It should be noted that such macroscopic theories depend on the notion that a meniscus has a fixed and stable periphery. On the contrary, our Monte Carlo simulations have revealed that a nanometer-sized meniscus often shows large fluctuations in its periphery and can be unstable.<sup>6,7</sup> Another common notion in conventional theories of capillary force is that the tip and sample surfaces are smooth. Any real materials however tend to have some roughness, especially at the atomic scale. Herein, we investigate the effect of atomic-scale tip roughness on the capillary force by using Monte Carlo simulations.

Our simulations are based on a lattice gas model.<sup>8,9</sup> To study collective phenomena involving phase transitions and coexisting phases, the lattice gas model has been a standard method. This captures the essential features of capillary condensation without requiring the molecular details of water. Our use of a lattice model is also strongly supported by its success in explaining the phase behavior of nanoscale confined water.<sup>10</sup> For a carbon nanotube (1.3 nm long) immersed in water, Maibaum and Chandler<sup>10</sup> found that the lattice model is fully consistent with an atomistic simulation.<sup>11</sup> Our previous lattice model calculation also reproduced the typical magnitude of the experimental pull-off force and its humidity dependence.<sup>8</sup> Therefore, we will use the lattice model to draw qualitative conclusions concerning the capillary force.

The system geometry is chosen to imitate a hemispherical AFM tip above a flat sample surface.<sup>6,8</sup> The flat sample surface is a square lattice located at  $Z = 0$ . Water molecules can occupy cubic lattice sites confined between the tip and sample. Here lengths are in units of the lattice spacing,  $l$ . In physical

dimensions, the lattice spacing is taken to be the molecular diameter of water, 0.37 nm.<sup>10</sup> The horizontal range of our system is  $-30 \leq x, y \leq 30$ . Only the first quadrant ( $x \geq 0, y \geq 0$ ) of the system is simulated by using a Monte Carlo method, and the remaining quadrants are taken to be mirror images of the first with respect to the  $XZ$  and  $YZ$  planes, and the  $Z$  axis.

Figure 1 illustrates four different tips that were studied. The tip labeled A is a smooth spherical tip, and Figures 1B–D correspond to rough tips. The surface of the smooth tip (Figure 1A) is defined as the collection of cubic lattice sites closest to a spherical surface with a radius of 30 lattice spacings (11 nm). Due to the small scale of the roughness, the tips are not much different from each other. We have chosen this set of tips to study the effects of atomic-scale roughness which seems inevitable in any AFM experiment. We show later that a small change in the tip shape leads to a remarkable difference in the capillary force.

In the Monte Carlo calculations, the intermolecular and molecule–surface interactions are nearest-neighbor types: a water molecule interacts with its nearest neighbor molecules with an attraction  $\epsilon$  and has its own chemical potential  $\mu$ . When it is located at one of the nearest-neighbor sites of the tip and sample surfaces, it feels binding energies,  $b_T$  and  $b_S$ , respectively. We can write the system Hamiltonian as

$$H = -\epsilon \sum_{i,j=\text{nn}} c_i c_j - b_T \sum_{i=\text{tip}} c_i - b_S \sum_{i=\text{sample}} c_i \quad (1)$$

where  $c_i$  is the occupation number (1 or 0) of the  $i$ th site, and the first summation runs over nearest-neighbor pairs, the second is for the sites on the tip surface, and the third for the sample surface sites. Using the Hamiltonian above, we performed grand canonical ( $\mu VT$ ) Monte Carlo simulations by following a procedure detailed elsewhere.<sup>8,9</sup> The relative humidity (RH) is defined as  $\exp[(\mu - \mu_c)/k_B T]$ , where  $\mu_c (= -3\epsilon)$  is the chemical potential at the bulk gas–liquid transition.<sup>12</sup> Temperature in our simulation is 300 K. Simulation results are converted to quantities with physical units as described in ref 8. Energetic parameters,  $b_T/\epsilon$  and  $b_S/\epsilon$ , are chosen to mimic a silicon-nitride

\* Corresponding authors. E-mail: jkjang@pusan.ac.kr; schatz@chem.northwestern.edu.

<sup>†</sup> Pusan National University.

<sup>‡</sup> Northwestern University.

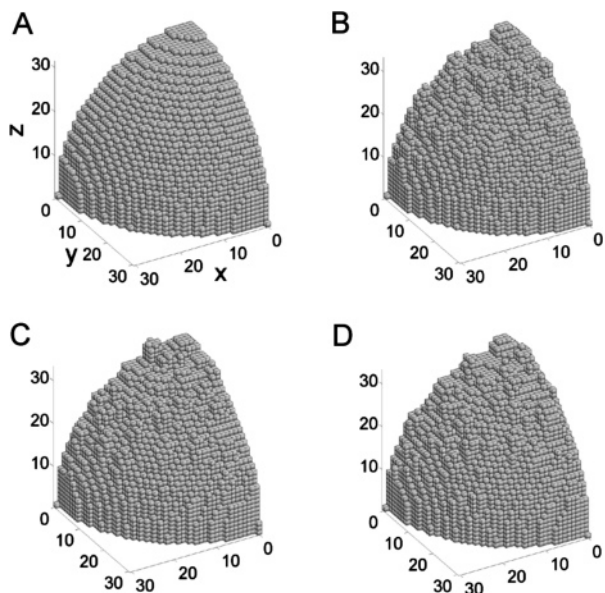


**Figure 1.** Four different tips examined in our simulations. The figure shows a smooth spherical tip (A) and 3 rough tips (B, C, and D). Tip surface sites are represented as cubes. Lengths in the figure are in units of the lattice spacing,  $l$  ( $= 0.37$  nm) and the tip radius is 30 lattice spacings (11 nm). Only the first quadrant ( $x \geq 0, y \geq 0$ ) of our system is shown. The tip is drawn upside down for visual clarity. The root-mean-square (rms) roughness for tips B, C, and D is 0.22 nm, 0.21 nm, and 0.19 nm, respectively. The roughness here is defined as the rms deviation of the  $Z$  positions of the rough surface sites from those of the smooth surface sites, A.

tip interacting with mica. The tip binding energy,  $b_T$ , is taken from the heat of adsorption of a water molecule on a silicon-nitride tip (50 kJ/mol).<sup>13</sup> The water–mica binding energy,  $b_S$ , is taken from the ab initio calculation by Odell et al. (46 kJ/mol).<sup>14</sup> Dividing the above values by a water–water hydrogen-bond strength (18.63 kJ mol<sup>-1</sup>)<sup>15</sup> gives  $b_T/\epsilon = 2.68$  and  $b_S/\epsilon = 2.47$ .

The capillary force,  $F$ , at a given tip–sample distance,  $h$ , is calculated by using the following relation,<sup>16</sup>

$$\left(\frac{\partial F}{\partial \mu}\right)_{h,T} = \left(\frac{\partial N_{\text{ex}}}{\partial h}\right)_{\mu,T} \quad (2)$$

where  $N_{\text{ex}}$  is the excess number of molecules with respect to bulk ( $N_{\text{ex}} = N - N_{\text{bulk}}$ ). The capillary force  $F(h)$  is obtained by integrating eq 2 with respect to  $\mu$ . Starting from a sufficiently low  $\mu$ , we numerically integrate eq 2 by evaluating  $(\partial N_{\text{ex}}/\partial h)$  at intermediate  $\mu$  values. We calculate the bulk density ( $\rho = N_{\text{bulk}}/V$ ,  $V = \text{volume}$ ) by using mean-field density functional theory (DFT).<sup>17</sup> We checked the validity of DFT by running several simulations for the bulk system, and quantitative agreement with Monte Carlo simulations was found.

In Figure 2, we plot the capillary force,  $F(h)$ , for the four tips shown in Figure 1. The force–distance curve is drawn for two representative RHs of 11% (left, Figure 2) and 79% (right, Figure 2). Typically,  $F(h)$  is attractive ( $F < 0$ ) when the tip is close to the sample ( $h < 2$  nm). As  $h$  increases,  $F(h)$  eventually approaches zero. The figure shows that the range of  $F(h)$  increases as RH rises. Remarkably, depending on the tip shape, the force can differ by several nN in magnitude (the largest difference is  $\sim 8$  nN at RH = 79%, see the right panel of Figure 2). In most cases,  $F(h)$  minimizes at  $h = 2l$ . Tip B at low RH ( $< 40\%$ ) however has a force minimum at  $h = l$ . At RH above 40%, all the tips show a qualitatively similar dependence of

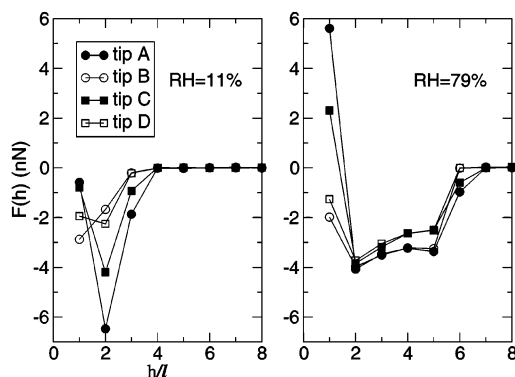


**Figure 2.** Capillary force  $F$  vs. the tip–sample distance  $h$  at a low- and a high- relative humidity (RH). For tips A–D in Figure 1, the force–distance curve is drawn for RHs of 11% (left) and 79% (right). The distance unit is the lattice spacing,  $l$ , and the force unit is nN. The forces for tips A, B, C, and D are drawn as filled circles, open circles, filled squares, and open squares, respectively. Lines are drawn for a guide to eyes. A negative (positive)  $F(h)$  corresponds to an attractive (repulsive) force on the tip.

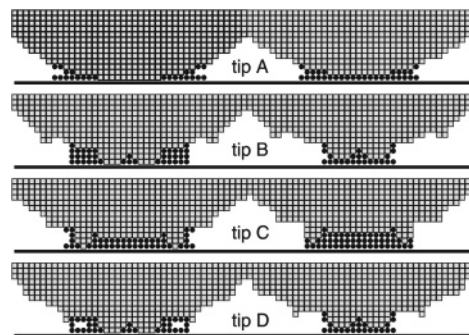


**Figure 3.** Water meniscus structures for the tips in Figure 1 at RH = 11%. For tips A (top), B (upper middle), C (lower middle), and D (bottom) in Figure 1, we show the liquid profiles at  $h = l$  (left) and  $h = 2l$  (right). For visual clarity, we took a 2-dimensional cross section (the  $XZ$  plane) of the liquid profile (drawn as filled circles) near the tip end ( $-20l \leq x \leq 20l, 0 \leq z \leq 13l$ ). Tip sites are drawn as gray squares, and the sample surface as solid lines.

$F(h)$  on  $h$  (right, Figure 2). Overall,  $F(h)$  for each tip is quite different at low RH but becomes similar at high RH.

We next examine the meniscus structure that gives rise to the capillary force in Figure 2. In Figure 3, we plot the liquid profile (drawn as filled circles) for each tip at RH = 11%. Here, the liquid profile is defined as a collection of lattice sites with an average occupancy above 1/2.<sup>7</sup> For visual clarity, we only show a 2-dimensional cross section (the  $XZ$  plane) of the liquid profile near the tip end. For each tip, we have drawn the liquid profiles at  $h = l$  (left, Figure 3) and  $h = 2l$  (right, Figure 3). One can see that, at the low RH, the meniscus is small and responds sensitively to the atomic-scale roughness of the tip. The capillary force is dominated by the accumulation of liquid around a single or a small number of asperities. As RH increases, the meniscus starts to cover up many asperities, and then it depends only on overall tip curvature. At 79% RH, the meniscus is largely independent of small-scale roughness. Unlike for a macroscopic tip, however, the atomic-scale roughness still plays a role in the sense that the capillary forces for our nanoscale tips never become identical.

Notice, in Figure 2, the capillary force can be repulsive ( $F(h) > 0$ ): for tips A and C at RH = 79%, the force is repulsive when the tip is in contact with the sample,  $h = l$ , (right, Figure 2). Why? First note the force,  $F(h)$ , is determined by the change in the grand potential,  $\Omega(h + l) - \Omega(h)$ , that occurs when the

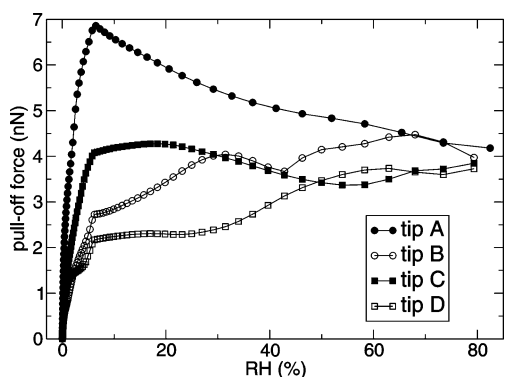


**Figure 4.** Pull-off force vs relative humidity (RH) for the smooth tip (tip A) and three rough tips (tips B, C, and D) in Figure 1. The pull-off forces of the tips A, B, C, and D are drawn as filled circles, open circles, filled squares, and open squares, respectively. Lines provide a visual guide.

tip-sample distance  $h$  increases by one lattice spacing  $l$ .<sup>9</sup> An attractive  $F(h) (< 0)$  means that the system is more stable (lower value in  $\Omega$ ) at the tip-sample distance of  $h$  than at the distance of  $h + l$ . This occurs in most cases because, as  $h$  decreases, the liquid gets more confined between the tip and sample surfaces, and thus it feels stronger surface fields. One should note, however, that decreasing  $h$  from  $2l$  to  $l$  squeezes molecules out of the confined space between the tip and sample. That is, molecules just cannot exist at the tip-contact area defined as the area where the tip surface contacts the sample surface. At low RHs, this “squeezing-out” of liquid is not substantial and can be compensated by the increased surface fields due to a higher degree of confinement. At high RHs, such as 79%, the number of molecules lost during the squeezing can be substantial depending on the tip shape (445 and 335 for tips A and C, respectively). Due to random variations in tip structure, tips A and C have larger tip-contact areas than those of tips B and D (see Figure 1 instead of Figure 3 which shows only 2-dimensional cross sections of tips). This substantial loss in the number of liquid molecules means a significant reduction in cohesive energy of the confined liquid. As a result, the tip-contact distance,  $h = l$ , is not favorable (a higher  $\Omega$ ) compared to  $h = 2l$ . Correspondingly, the capillary force is repulsive at  $h = l$ . Experimentally, the force on the tip eventually becomes repulsive as the tip approaches a sample (due to the electron-electron repulsion between atoms). Interestingly, our simulation shows that the capillary force itself can be repulsive between two completely wetting<sup>12</sup> surfaces (within our lattice gas model, a surface is completely wetting if its binding energy  $b$  is larger than  $\epsilon$ ). The Kelvin equation, on the other hand, always predicts an attractive capillary force between two completely wetting surfaces.<sup>5</sup>

We finally examine pull-off forces of the four tips in Figure 1. The pull-off force is defined as the magnitude of force needed to pull away a tip initially in contact with the sample. To obtain the pull-off force for a given humidity, we calculated  $F(h)$  as in Figure 2 for each tip. We identified the magnitude of the most attractive force in the  $F(h)$  curve as the pull-off force. In Figure 4, the pull-off force of each tip is plotted as a function of RH. By and large, the pull-off force of a rough tip is smaller than that of the smooth tip. It is remarkable that a slight difference in tip shape leads to a drastic difference in the pull-off force. The effect of roughness is greater at low humidities. For example, at humidity 6.5%, the pull-off force of the smooth tip (6.9 nN) is 3 times larger than that of tip D (2.3 nN). As humidity approaches 80%, the roughness effect gets smaller. As discussed above, this is due to the fact that the size and

shape of the small-scale menisci are sensitive to the atomic-scale roughness of the tip. Why is the pull-off force larger for the smooth tip, especially at low RHs? Again, we need to look into the underlying meniscus structure as in Figure 3. Notice the pull-off force in most cases is the force at  $h = 2l$ . At low RHs, the meniscus at this distance is laterally confined near the tip end as shown in Figure 3, and the force is mainly governed by the number of molecules directly sandwiched between the tip and sample surfaces. As the nearest neighbors of both the tip- and sample-surface sites, these molecules feel strong attractions (2.5 times stronger than the intermolecular interaction) from both the tip and the sample. The number of these molecules, in turn, is determined by the contact area (see above for definition) of each tip. The smooth tip A has the largest contact area (87 lattice points) among all the tips and thus there are more molecules directly sandwiched between the tip- and sample- surface sites. Therefore, the force at  $h = 2l$  is the most attractive for the smooth tip, giving the largest pull-off force. Similarly, tip C has a larger tip-contact area (53 lattice points) than that of tip D (19 lattice points), and its pull-off force is generally larger than that of tip D (Figure 4). Why is the pull-off force of tip B (with the smallest contact area of 15 lattice points) larger than that of tip D? Unlike other tips, the force minimum occurs at  $h = l$  for tip B at low RHs (<40%). At this distance, there is no molecule directly sandwiched between the tip and sample surfaces. However, tip B, having the largest surface roughness, has more rifts than other tips. Therefore, more molecules can be trapped by these rifts for tip B. It turns out that, at low RHs, tip B traps more liquid molecules at  $h = l$  than at  $h = 2l$ . An increased number of molecules trapped in the rifts means an enhanced intermolecular cohesion as well as an increased attraction from the tip surface. This additional stabilization in energy for tip B is big enough to give a stronger pull-off force on tip B than on tip D. The above analysis shows that arrangement, as well as size, of the tip contact area is important in determining the pull-off force. When the tip contact sites are scattered and there are significant rifts between them, liquid molecules can fill in the rifts, leading to a substantial increase in the force. Therefore, we need to look closely at the tip shape in order to understand the pull-off force calculated in the simulations.

One can see that, depending on the tip shape, the pull-off force in Figure 4 varies with humidity in a radically different way. As humidity rises from zero, the pull-off force of the smooth tip (Figure 1A) quickly increases to reach a maximum at a humidity 6.5% and then gradually decreases. For rough tips (B–D of Figure 1), we also observe a rapid increase of the force as humidity increases from zero to 6.5%. As humidity further grows from 6.5%, the pull-off force for the rough tips slowly increases, instead of decreasing. For the tips B and C, the pull-off force shows alternating maxima and minima with rising humidity. The pull-off force of tip D is mostly a monotonically increasing function of humidity. Interestingly, with slight changes in the tip shape, our simulations qualitatively reproduce both the monotonic<sup>1,2</sup> and nonmonotonic<sup>3</sup> dependence of the experimental pull-off force on humidity (for a silicon nitride tip on a mica surface). A quantitative comparison with experiment however seems difficult considering the limitations of our lattice gas model and the unknown tip shape used in experiment.

In summary, unlike its macroscopic counterpart, a nanoscopic meniscus in AFM gives rise to a capillary force that is sensitive to the atomic details of the tip geometry. Determination of the tip geometry is thus needed in order to determine how the pull-

off force depends on humidity. Overall, tip roughness reduces the magnitude of the pull-off force, with greater effect at low humidities (0–30%). What will be the effects of the sample (mica) roughness? We found, for a smooth tip, a rough mica surface gives pull-off forces smaller than those for a flat one. As with the tip roughness, this sample roughness effect is significant at low humidities (<30%). The details of this, as well as an investigation of tips and samples with various roughness, will be reported elsewhere.

**Acknowledgment.** J.J. gratefully acknowledges the funding from KRF Grant No. R05-2004-000-10484-0 and Pusan National University Grant-2003. G.C.S. and M.A.R. were supported by AFOSR MURI Grant F49620-00-1-0283 and by the National Science Foundation.

### References and Notes

- (1) Sedin, D. L.; Rowlen, K. L. *Anal. Chem.* **2000**, *72*, 2183.
- (2) Thundat, T.; Zheng, X. Y.; Chen, G. Y.; Warmack, R. J. *Surf. Sci. Lett.* **1993**, *294*, L939.
- (3) Hu, J.; Xiao, X. D.; Ogletree, D. F.; Salmeron, M. *Science* **1995**, *268*, 267.
- (4) Fisher, L. R.; Israelachvili, J. N. *J. Colloid Interface Sci.* **1981**, *80*, 528.
- (5) Orr, F. M.; Scriven, L. E.; Rivas, A. P. *J. Fluid Mech.* **1975**, *67*, 723.
- (6) Jang, J.; Schatz, G. C.; Ratner, M. A. *Phys. Rev. Lett.* **2004**, *92*, 085504.
- (7) Jang, J.; Schatz, G. C.; Ratner, M. A. *J. Chem. Phys.* **2002**, *116*, 3875.
- (8) Jang, J.; Schatz, G. C.; Ratner, M. A. *J. Chem. Phys.* **2004**, *120*, 1157.
- (9) Jang, J.; Schatz, G. C.; Ratner, M. A. *Phys. Rev. Lett.* **2003**, *90*, 156104.
- (10) Maibaum, L.; Chandler, D. A. *J. Phys. Chem. B* **2003**, *107*, 1189.
- (11) Hummer, G.; Rasaiah, J. C.; Noworyta, J. P. *Nature* **2001**, *414*, 188.
- (12) Pandit, R.; Schick, M.; Wortis, M. *Phys. Rev. B* **1982**, *26*, 5112.
- (13) Fubini B.; Volante, M.; Bolis, V.; Giamello, E. *J. Mater. Sci.* **1989**, *24*, 549.
- (14) Odellius, M.; Bernasconi, M.; Parrinello, M. *Phys. Rev. Lett.* **1997**, *78*, 2855.
- (15) Grabowski, S. J. *Chem. Phys. Lett.* **2001**, *338*, 361.
- (16) Ash, S. G.; Everett, D. H.; Radke, C. *Faraday Trans. 2* **1973**, *69*, 1256.
- (17) De Oliveira, M. J.; Griffiths, R. B. *Surf. Sci.* **1978**, *71*, 687.